JOURNAL OF MARITIME RESEARCH

Vol XXIII. No. II (2026) pp 202–216

ISSN: 1697-4840, www.jmr.unican.es

Numerical Analysis of Ship Hull Structure under Bulbous Bow Collision: Influence of Bow Shape and Impact Velocity on Structural Integrity

Md. Ashraful Islam Opi[1], Kazi Naimul Hoque[2,*]

ARTICLE INFO

Article history:
Received 05 Jul 2025;
in revised from 17 Jul 2025;
accepted 28 Aug 2025.

Keywords:
Ship Collision, Hull Damage, Side Shell Structure, Finite Element Analysis, Bulbous Bow.

ABSTRACT

This paper presents a comprehensive finite element analysis (FEA) of a ship's side shell structure under the influence of a bulbous bow collision. The geometry of the forwardmost portion of the bulbous bow of the striking ship is simplified into four different shapes – spherical, cylindrical with hemispherical end, trapezoidal prism and wedge shape – to investigate the structural damage and determine the effective bulbous bow shape in terms of structural integrity of the side shell under the impact of the bulbous bow during collision. Several collision scenarios are simulated varying the collision velocities and bulbous bow shapes and validated with analytical results using two different analytical methods. The analysis yields critical information regarding reaction forces, penetrations and energy absorptions. The numerical results show good agreement with the analytical findings, particularly until crack initiation into the hull structure. The spherical shape is found to be the more effective bulbous bow shape, as determined by the maximum energy absorbed and reaction forces exerted by the side shell against the impact of the bow during penetration until fracture into the hull structure.

© SEECMAR | All rights reserved

1. Introduction.

Historically, maritime incidents involving collisions have had far-reaching consequences, leading to loss of life, environmental damage and economic losses. Ship collisions can occur in various forms, depending on the speeds, angles, points of impact and relative positions of the vessels involved. There is a higher probability that a ship may have a major collision strike over her lifespan as sea channels are getting more crowded and ship speeds are rising [1]. The European Maritime Safety Agency recently released its annual overview of marine casualties and incidents. It stated that the most common cause of casualties between 2014 and 2022 is collisions, accounting for 21.6% of all incidents. Between 2010 and 2020, collisions accounted for the majority of medium-sized (between 7 and 700 tonnes) and big (above 700 tonnes) oil spills. Furthermore, collisions and grounding were the cause of 62% of these spills from 1970 to 2023. Approximately 2,000 tonnes of oil were lost to the marine environment in 2023, despite the fact that the total amount of oil lost from tanker spills was the second lowest annual total in the previous 50 years.

In addition to operational and environmental factors, structural topology can have an impact on a ship's dynamic reaction after a grounding or collision [2], [3], [4]. The bulbous bow, an extension of a ship's hull, is mostly designed to enhance the hydrodynamic performance of a ship by reducing wave-making resistance. However, in the event of a collision, the bulbous bow can exert significant forces on the impacted structure which potentially leads to structural damage or failure [5]. Particularly when they happen close to coastal areas or small canals, collisions of hazardous substance carriers like oil tankers, LNG/LPG can pose major environmental concerns [6], [7]. The collision between the bulbous bow and the side shell referred as Bow-to-Side collision can cause substantial damage

[1]Department of Naval Architecture and Offshore Engineering, Bangladesh Maritime University, Dhaka, Bangladesh. E-mail Address: ashraful.islam.opi.99@gmail.com.

[2]Department of Naval Architecture and Marine Engineering, Bangladesh University of Engineering and Technology, Dhaka, Bangladesh. E-mail Address: kazinaim@name.buet.ac.bd.

[*]Corresponding author: Kazi Naimul Hoque. E-mail Address: kazinaim@name.buet.ac.bd.

to both the bow and side shell structures [8], [9]. It is vital to precisely model the structural reliability of the ships involved in the accident, including the impact strength and level of damage, in order to prevent such consequences. One of the main concerns with the prospective design criteria is determining the precise level of damage to the ship structures that are subject to impact loadings. Experiments, finite element simulations, empirical formulas, and simplified analytical techniques are utilized to evaluate the underlying mechanics of impacted structure [10], [11], [12]. As real-life experiments are constrained by various limitations and complexities, the utilization of finite element analysis has emerged as a valuable tool. It facilitates the assessment of impact force, energy absorption, and the extent of damage incurred by the impacted structure in collision scenarios. This computational approach offers advantages in terms of flexibility, cost-effectiveness, and the ability to simulate diverse collision scenarios with precision and reliability. For instance, the energy absorbed during a collision and the degree of damage resulting from significant in- and out-of-plane loadings in the hull structures have been determined using extensive finite element models of ship structures [1], [13], [14], [15], [16]. Particularly, the nonlinear finite element method (NFEM) has been regarded as an effective and practical technique for more accurate calculations of the structural crashworthiness in ship crashes [13], [17], [18]. Non-linear finite element method can precisely produce a structural impact response without fracture with the real material properties and boundary conditions [19], [20], [21].

Figure 1: Damage in the RoPax Vessel URD [13].

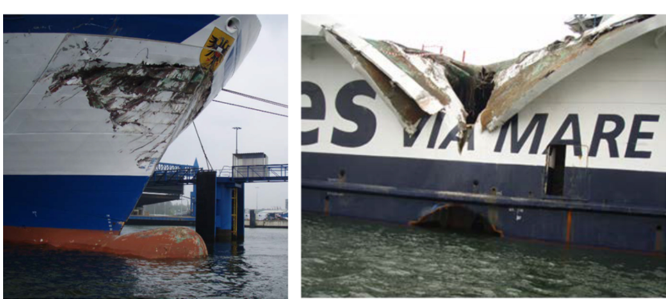

Source: Authors.

As maritime transportation evolves, there's a notable trend toward larger ship sizes, necessitating the advancements in structural design to accommodate these changes. Larger vessels are typically constructed using longitudinal framing techniques, emphasizing the use of longitudinal members such as stiffeners to enhance structural integrity of the vessel. However, existing experimental and numerical analyses of ship hull structures during collisions predominantly focus on vessels with longitudinal and combined framing configurations [11], [17], [22], [23]. The impact responses of ship side shells during collisions with bulbous bows are also evaluated highlighting the importance of stiffeners in enhancing crashworthiness [24]. Contrastingly, smaller to medium-sized ships, including inland vessels, typically employ transverse framing structures, with limited incorporation of longitudinal elements. These vessels are particularly prone to collisions due to the narrow confines of inland waterways and the dense maritime traffic they navigate. Therefore, there's a pressing need to investigate the structural behavior of the side shell of these vessels to accurately predict the extent of damage and failure resulting from severe collisions.

This research paper aims to investigate the penetration depth, impact resistance and energy absorption of double hull structure of a medium sized ship which is subjected to collision with the bulbous bow of another ship. The struck ship's failure behaviour and plastic deformation are significantly influenced by the striking bow's geometry [1], [25]. To assess the structural damage and deformation characteristics of the ship side shell under bulbous bow collision, a finite element (FE) approach was employed to capture the complex stress-strain behavior and failure progression. The methodology builds upon established finite element strategies for modeling irregular domains and unstructured meshes, which are crucial in capturing the geometric complexity of ship structures and collision interfaces [26]. For numerical analysis aimed at determining the structural failure of the impacted structure, it is feasible to simplify the complex geometry of the bulbous bow shape retaining key features essential for accurately predicting structural responses during collision events [13], [27], [28]. This simplification approach involves representing the bulbous bow shape using simplified geometric shapes. Four different shapes i.e. Spherical, Cylindrical with Hemispherical End, Trapezoidal Prism and Wedge are used in order to identify the most effective simplified bulbous bow shape in terms of structural damage. This research is important for improving safety measures and informing the design and construction of inland vessels, ensuring their resilience against collision events in challenging operating environments. The knowledge can lead to the implementation of targeted safety, ultimately reducing the risk of structural failures and potential disasters at sea.

2. Model and Geometry.

2.1. Finite Element Model.

In this paper ABAQUS software is used to build four finite element models of a double hull structure subjected to collisions with bulbous bows. Dynamic analysis, often known as time-history analysis, is carried out to investigate how the structure will react dynamically to any kind of broad time-dependent stress. In the inner plate, fixed support is applied for the analysis.

Initially the collision is taken as a sharp Bow-to-Side collision which presents the striking ship directly hit the struck ship at an angle of 90 degrees and the striker is regarded as a stiff structure. The ship collision scenario is represented by the numerical simulations conducted by the ABAQUS CAE software. The outer shell of a double-hull general cargo ship is struck by a stiff bulbous bow of a striking ship (Fig. 2).

The geometry of the side shell structure of the reference ship is shown in Fig. 3. and Table 1 lists the reference ship's primary dimensions. The model has a double-hull and a double-bottom structure. The double-hull comprises fifteen frames,

Figure 2: Bulbous bow to ship side collision scenario.

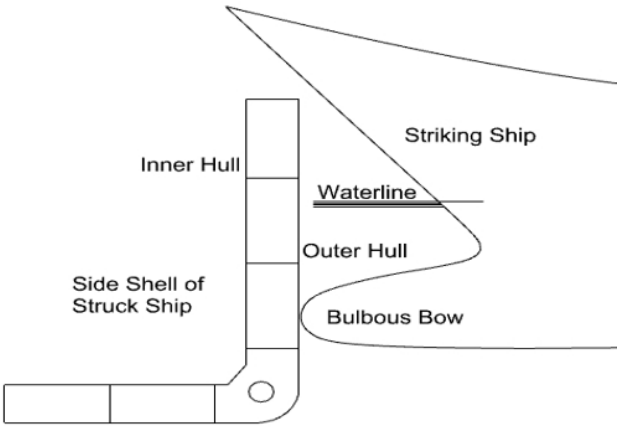

Source: Authors.

three stringers, one inner panel, and one outer panel. The bottom structure includes two girders, one outer bottom and one inner bottom.

Figure 3: Dimension of the side shell structure.

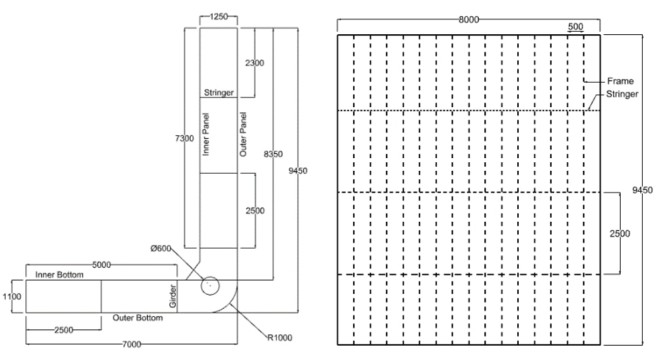

All units are in mm.
Source: Authors.

Figure 4: Finite element model of the side shell structure of the struck ship.

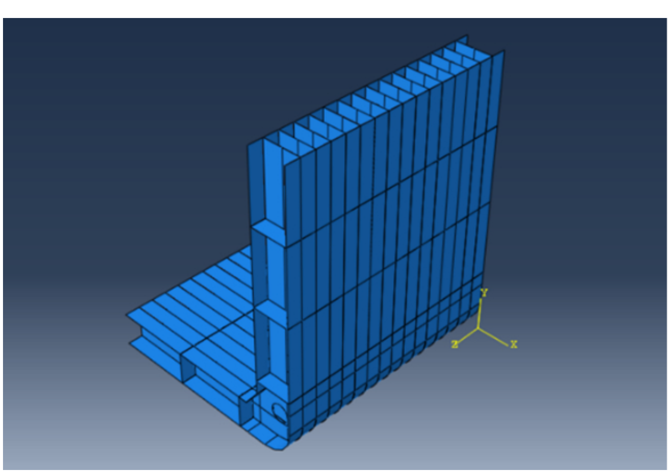

Source: Authors.

The collision event is assessed using dynamic explicit method for numerical simulations, in which the double bottom construction of the model is bounded by three girder spacings, and the double hull structure is restricted by three stringer spacings along the vertical direction and sixteen frame spacings along the longitudinal direction (Fig. 4). The frame spacings and the stringer and girder spacings are 500 mm and 2500 mm respectively. The plate thickness of both inner and outer panel is 10 mm, the plate thickness of the frames is 14 mm, the plate thickness of stringer and girder is 12 mm. The height of frames and stringer is 1.25 m indicated in Table 2.

Table 1: Main particulars of the struck ship.

Length Overall	90 m
Length Between Perpendicular	85 m
Breadth Moulded	14 m
Draught Moulded	6.1 m
Depth Moulded	9.45 m
Deadweight	4868 tonnes

Source: Authors.

Table 2: Scantlings of the finite element model.

Frame Spacing	500 mm
Stringer Spacing	2500 mm
Girder Spacing	2500 mm
Frame Height	1250 mm
Double Bottom Height	1100 mm
Frame Thickness	14 mm
Outer & Inner Plate Thickness	10 mm

Source: Authors.

Structural response mostly depends on the forwardmost geometry of the bulbous bow in case of ship collision scenario. The forwardmost part of the bulbous bow can be compared with some simplified geometry to evaluate the impact response of the ship hull structure against these striking bows. The more accurate result can be obtained by generating the existing different bulbous bow models. Hence the simplified shapes are designed to evaluate the structural behavior of the ship hull structure. The model of each part was generated according to their respective geometry and dimensions and assembled together to give it a shape close to the real scenario. To assess the resistance of struck structure conservatively, the striking bow is considered to be rigid. Four distinct shapes are chosen for the evaluation in order to identify the effective shape of bulbous bow. The shapes modelled for the analysis are hemispherical, trapezoidal prism, wedge, and cylinder with hemispherical ends. The models generated for the analysis are shown in Fig. 5. These four distinct forms' cross-sectional areas were maintained almost equal. The final supporting requirement was given as fixed. Table 3 shows the dimensions of these simplified striking bows. The finite element models incorporated with both the side shell and striking bows are presented in Fig. 6.

Figure 5: Simplified shapes of striking bow.

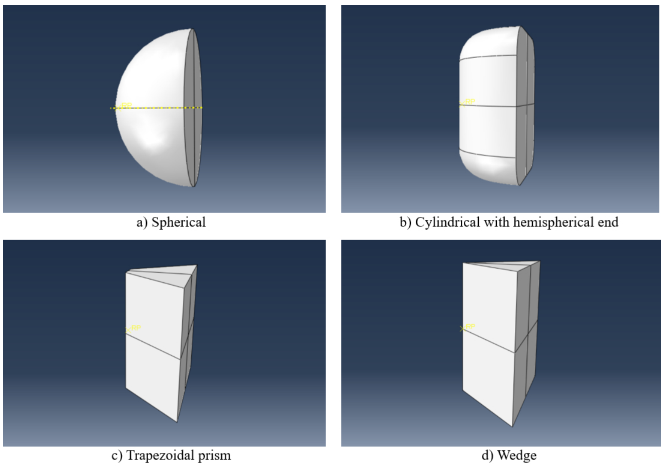

Source: Authors.

Table 3: Dimensions of the simplified bow shapes.

Model Name	**Dimension**
Hemispherical	750 mm (Diameter)
Cylinder with hemispherical end	1500 mm × 750 mm
Trapezoidal Prism	1500 mm × 750 mm × 250 mm
Wedge	1500 mm × 750 mm

Source: Authors.

2.2. Material.

Fig. *6*. Bulbous bows in contact with the side shell structure

For energy absorption collision assessments, the material properties are crucial parameters. These parameters include yield stress σ_y, ultimate tensile stress σ_u, and elongation at break ε_f also referred to fracture strain or rupture strain. According to research done on materials data from the shipbuilding sector the ultimate tensile stress of the materials has a significant influence on the rupture strain [13]. Typically, as the ultimate tensile stress of a material rises, its rupture strain tends to decrease. The choice of materials has a direct impact on the strength and cost of the ship. Hence it is crucial in structural design. Mild steel and higher-strength steel are commonly used in the construction of hull structures due to their exceptional properties including high strength, adequate ductility, and cost-effectiveness [29]. When a material undergoes large deformations, it tends to become harder, meaning it resists further deformation more strongly. This hardening behavior plays a crucial role in ductile fracture, as it influences how the material deforms and ultimately fails when subjected to excessive loads. For a certain stress states, such as uniaxial tension and equi-biaxial tension, high-tensile strength steel AH36 shows higher ductility as compared to mild steel A [30]. Mild Steel Grade I is assigned as the material for both the shell structure and the bulbous bow to analyze the collision scenario, damage of the shell structure and energy absorption as well. Mild steel is highly weldable, allowing for efficient and secure joining of various components. This is essential in shipbuilding, where numerous sections and plates need to be seamlessly connected. Mild steel is widely available and can be sourced easily from various suppliers, making it a practical choice for shipyards. The properties of Mild Steel used for the analysis is given in Table 4.

Figure 6: Bulbous bows in contact with the side shell structure.

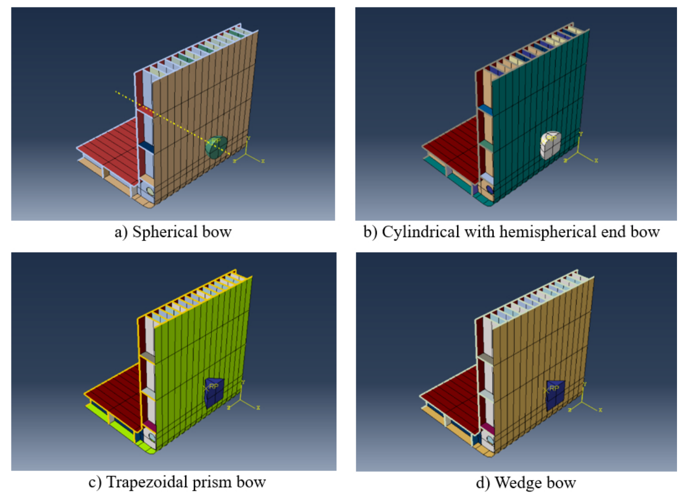

Source: Authors.

Table 4: Material Properties of the Model.

Material Used	Mild Steel Grade I
Density, (ρ)	7850 kg/m^3
Modulus of Elasticity (E)	210 GPa
Poisson's Ratio (ϑ)	0.29
Yield Strength (σ_y)	250 MPa
Ultimate Tensile Strength (σ_u)	410 MPa
Plastic Strain (ε)	0.23

Source: Authors.

In ship-ship collision analysis, it's commonly assumed that the bow of the striking ship is rigid, meaning it doesn't deform significantly upon impact [31]. This assumption simplifies the analysis by focusing solely on the energy absorbed by the ship being struck. The structural damage can be roughly estimated by assuming that the damage to the side shell of the struck ship is mostly confined around the rigid bow of the struck ship [13].

In previous studies on ship collision conducted using analytical method, the friction effect between the bow and impacted structure was not considered. Later in 2009, the friction coefficient was evaluated and measured by Karlsson et. al [32] and found that friction coefficient μ can have a magnitude of 0.23 which has been frequently used in several ship collision study in case of numerical simulations. Some finite element calculations have accepted the assumption that friction does not play a substantial role in ship collisions. A further investigation was conducted regarding the contribution of friction coefficient on energy absorption and revealed that the contribution is negligible when the penetration is small but it gradually increases as the penetration depth increases where the contribution is almost 10% in case of large penetration [13]. In this paper the friction coefficient is taken 0.3 for the analysis.

2.3. Inertia and Boundary Condition.

Both inertia and boundary conditions are fundamental aspects of any finite element analysis, ensuring that the numerical simulations accurately represent real-world scenarios and provide reliable engineering insights. When modeling dynamic events, it is essential to include inertia effects to properly account for the behavior of the structure under acceleration or deceleration. This involves defining the mass properties of the components, specifying the initial conditions, and selecting the appropriate analysis type. The inertia was applied at the reference point of the rigid bow which is basically the point where the mass of striking ship is concentrated and the point is in contact with the shell structure (Fig. 7a). Appropriate boundary conditions are crucial for accurately representing the physical behavior of the structure. It ensures that the model behaves realistically and provides meaningful results. The exposed edges of the structural component i.e. outer panel, inner panel, stringers, frames, girders are set fixed and no movement is allowed in any directions (Fig. 7b) so that the actual penetration of the bulbous bow can be obtained.

Figure 7: Boundary condition (a) bulbous bow; (b) entire structure.

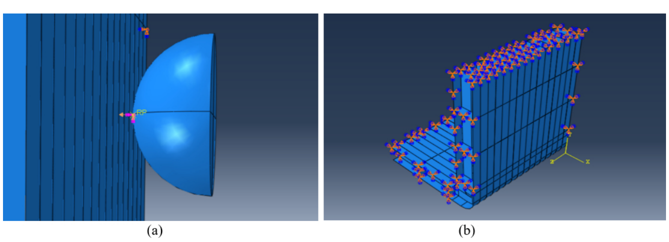

Source: Authors.

3. Finite Element Result.

A number of variables, including the relative displacements of the two ships, their speeds, the location of the collision, the angle of the collision, and the strength of their constructions, affect how much damage is done to them in a collision [33], [34], [35], [36]. Collison speed is one of the most important parameters which significantly influences the magnitude of structural damage and material failure of the structure subjected to dynamic loading [20], [37], [38]. According to statistics from real collisions, striking ships collide at an average speed of 4.27 knots, or 2.20 m/s [39]. The material's strain rate sensitivity can be ignored because of the relatively modest collision velocity [40]. For the study, four collision velocity i.e. 1.5 m/s, 2 m/s, 2.5 m/s and 3.0 m/s are taken and the Crushing Force, Strain Energy, Internal Energy and Total Energy are analyzed to determine the effective bulbous bow shape among four simplified shapes- Spherical, Cylindrical with Hemispherical End, Trapezoidal Prism and Wedge.

The striking bow is modeled by shell elements and an adequate offset of 250 mm is defined between the contact surface of the side shell structure and the bulbous bow. A rigid material is defined to ensure no deformation to the bulbous bow. The contact between the striking bow and the struck structure is defined as "Surface to Surface"; the friction coefficient is assumed at 0.3.

3.1. Results for 1.5 m/s collision velocity.

The collision is assumed to occur for 1 second and since the striking bow is rigid, so the bow can penetrate up to 1.25 m through the side shell structure. Fig. 8 and Fig. 9 depict the numerical forms of permanent deformation as well as the numerical force-displacement responses and absorbed energy-displacement curves of the double-hull structure subjected to various striking bows. Underneath the striker, the struck structure undergoes significant plastic deformation (Fig. 8). But because of the low collision velocity the struck ship does not experience a noticeable rupture at the outer panel and the inner hull of the side shell remains intact.

Figure 8: Double hull structure struck with different bow shapes at 1.5 m/s collision velocity.

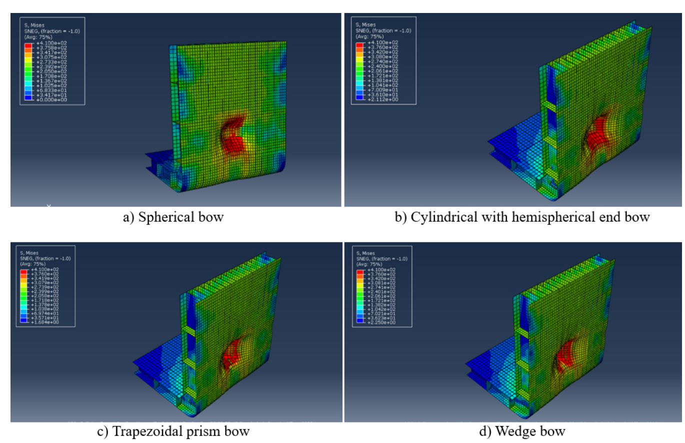

Source: Authors.

Because of the contact area with the struck structure, the striker's geometry has a significant impact on the failure mechanisms and structural plastic deformation. The instantaneous stiffness of the structure and the reaction force level are represented by the initial slope of the force-penetration curves (Fig. 9a). Additionally, it shows how resilient the structure is to impact loads and how long it can endure plastic deformation before fracture. For the structure affected by the wedge and trapezoidal prism striker, the slope is initially somewhat large. The spherical bow's slope is smaller than the other three, meaning that the structure needs less reaction force to resist the striking bow. The numerical simulation curve for energy vs displacement shows the energy absorption of the double hull structure under the impact of different shapes striking bulbous bow.

Since the bulbous bow is allowed to penetrate 1.25 m through the ship hull, no fracture occurs in this range for any of the simplified shape striking bow. The strain energy curve (Fig. 9b) for trapezoidal prism, cylindrical with hemispherical end and wedge shape bow noticeably fluctuate with the increase of penetration depth which indicates the greater risk of structural damage. Moreover, there is a rapid drop of energy in case of cylindrical, trapezoidal prism and wedge shape striking bow (Fig. 10b) when in contact with the bow. On the contrary, the energy absorption of the double hull structure is linear and consistent in case of spherical shape bulbous bow.

Figure 9: Numerical results of various striking bows at 1.5 m/s velocity.

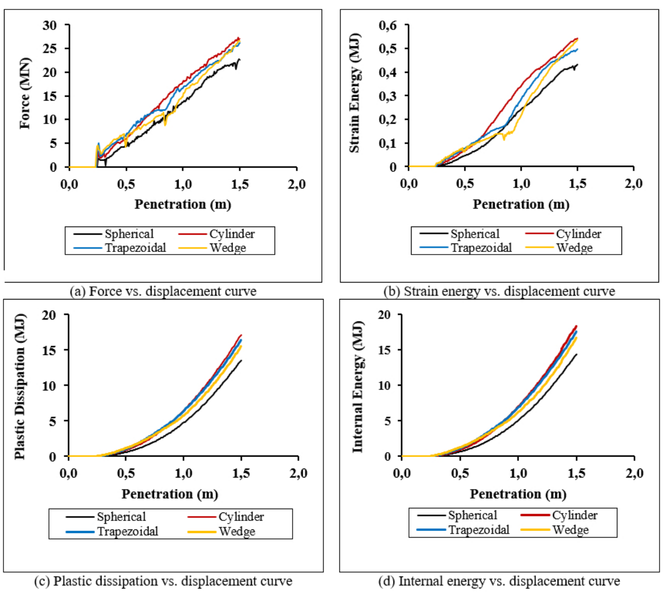

Source: Authors.

Fig 9c and Fig 9d illustrate the plastic dissipation and internal energy absorption of a ship side shell structure subjected to impacts by bulbous bows with different geometric shapes respectively. It is evident that the plastic dissipation and internal energy increases progressively with penetration depth for all bow shapes. The cylindrical bow exhibits the highest plastic dissipation, suggesting that it induces the most significant plastic deformation in the side shell structure. The trapezoidal and wedge-shaped bow follows closely, showing a slightly lower but comparable plastic dissipation. The spherical bow demonstrates the lowest plastic dissipation energy, indicating that it causes relatively less plastic deformation compared to the other shapes. The differences in energy dissipation can be attributed to the contact area and load distribution characteristics of the respective bow shapes. Despite the wedge-shaped bow having a smaller contact area, the crushing force and energy absorption curves exhibit improved performance in this case. This enhancement can be attributed to the alignment of the transverse frame beneath the outer plate, where the bow's edge impacts the frame perpendicularly to its thickness.

3.2. *Results for 2 m/s collision velocity.*

The deformation of the double-hull structure under the impact of different bulbous bow shapes at a collision velocity of 2 m/s reveals distinct structural responses based on the bow geometry (Fig 10). For the cylindrical, trapezoidal, and wedge-shaped bulbous bows, the deformation is more abrupt and rapid. These geometries concentrate the collision forces over a relatively smaller area, leading to localized stress intensification in critical structural components such as the outer plate, transverse frames, and stringers. This results in an earlier onset of cracks within the structure. The spherical bulbous bow exhibits a smoother and less abrupt deformation response. Its rounded geometry allows the collision forces to distribute across a broader area, reducing the localized stress intensity and delaying the onset of structural cracking. This broader force distribution minimizes the strain concentration in critical areas, enabling the hull to absorb more energy before experiencing significant damage.

Figure 10: Double hull structure struck with different bow shapes at 2 m/s collision velocity.

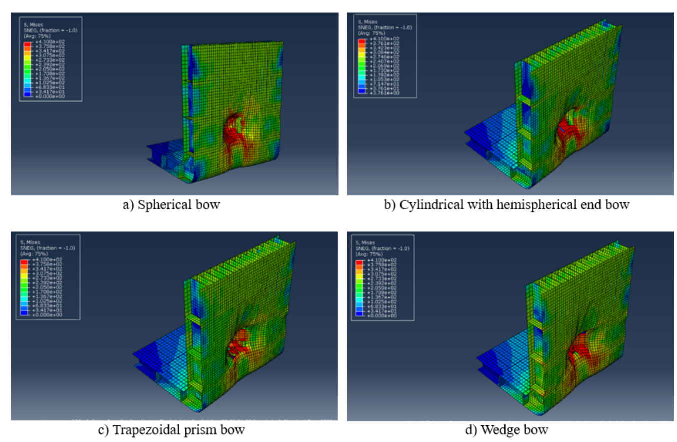

Source: Authors.

Fig. 11a illustrates the variation of reaction force with penetration depth for a ship's side shell structure when impacted by bulbous bows of different shapes at 2 m/s collision speed. For the wedge-shaped bow, the force curve shows sharper peaks followed by abrupt drops, indicating that its pointed geometry concentrates the impact force over a smaller area, leading to early crack initiation in the outer plate or transverse frames. In contrast, the cylindrical and trapezoidal bows generate smoother force curves, indicating a more uniform distribution of impact forces over a larger contact area. These shapes cause a delayed crack initiation compared to the wedge, as the structure has more capacity to absorb and redistribute the applied forces. The spherical bow demonstrates the lowest reaction force values overall, as its rounded shape distributes the force more evenly across the contact area. This reduces the likelihood of concentrated stress points and delays the onset of cracks, making it the least aggressive among the shapes in terms of damage initiation.

Figure 11: Numerical results of various striking bows at 2 m/s collision velocity.

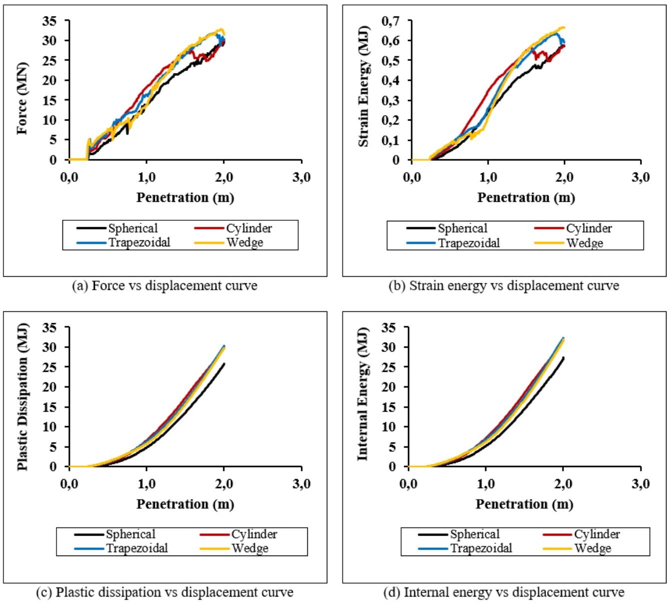

Source: Authors.

The strain energy curves for a collision speed of 2 m/s exhibit a trend consistent with those observed at a lower collision speed of 1.5 m/s (Fig 11b). This similarity suggests that the fundamental deformation and energy absorption mechanisms of the side shell structure remain comparable across these two collision velocities. While the total strain energy absorbed may vary due to the increased kinetic energy at 2 m/s, the overall pattern of how the structure deforms and absorbs energy does not significantly differ. The plastic dissipation (Fig 11c) and internal energy (Fig 11d) curves exhibit a steeper slope for cylindrical, trapezoidal and wedge shape bow, which refers a rapid accumulation of plastic dissipation and internal energy as penetration increases. In contrast, the spherical bow shape results in curves with a less steep slope, indicating a more gradual increase in plastic dissipation and internal energy with penetration.

Figure 12: Penetration depth at which crack occurs into the outer hull at 2 m/s collision velocity.

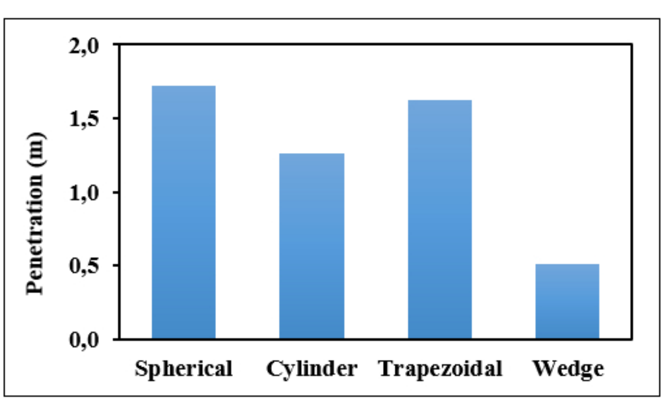

Source: Authors.

At a collision speed of 2 m/s, the bulbous bows are allowed to penetrate up to 1.75 m into the side shell structure. Within this penetration depth, the crack begins to form in the structure. Notably, the outer plate ruptures later when impacted by a spherical bow compared to other shapes. Fig 12 shows the penetration depth at which crack initiation occurs in the outer plate. The maximum reaction force and energy absorption of the structure leading up to the point of crack initiation for different bulbous bow shapes are illustrated in Fig. 13.

Figure 13: Maximum reaction force and absorbed energy before crack initiation at 2 m/s collision velocity.

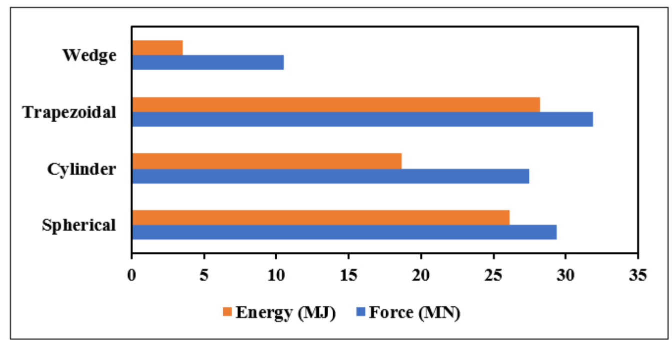

Source: Authors.

3.3. *Results for 2.5 m/s collision velocity.*

At a collision speed of 2.5 m/s, the bulbous bow penetrates up to 2.25 m into the side shell structure, resulting in notable deformation patterns in the ship hull. These deformations are illustrated in Fig 14 & Fig 15, which provides a detailed depiction of the structural response for different bulbous bow shapes.

Figure 14: Deformation of outer hull under the impact of different bows at 2.5 m/s collision velocity.

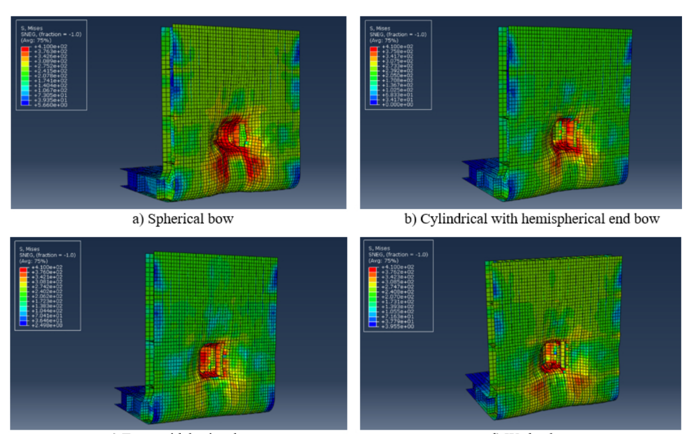

Source: Authors.

The observed deformation patterns at this collision speed closely resemble those at lower speeds, such as 1.5 m/s and 2 m/s which indicates a consistent response trend under varying impact velocities.

Figure 15: Deformation of inner hull under the impact of different bows at 2.5 m/s collision velocity.

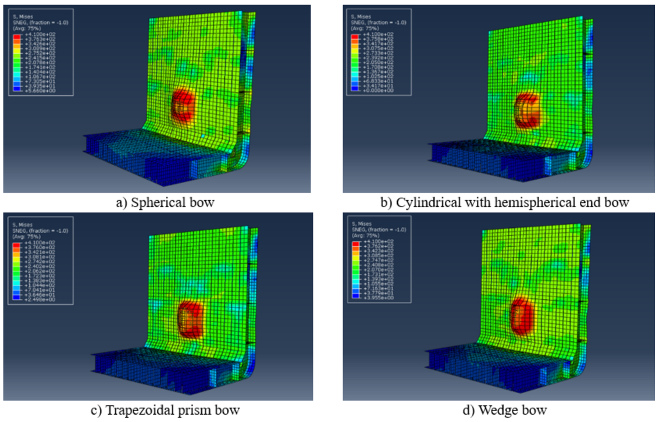

Source: Authors.

Figure 16: Numerical results of various striking bows at 2.5 m/s collision velocity.

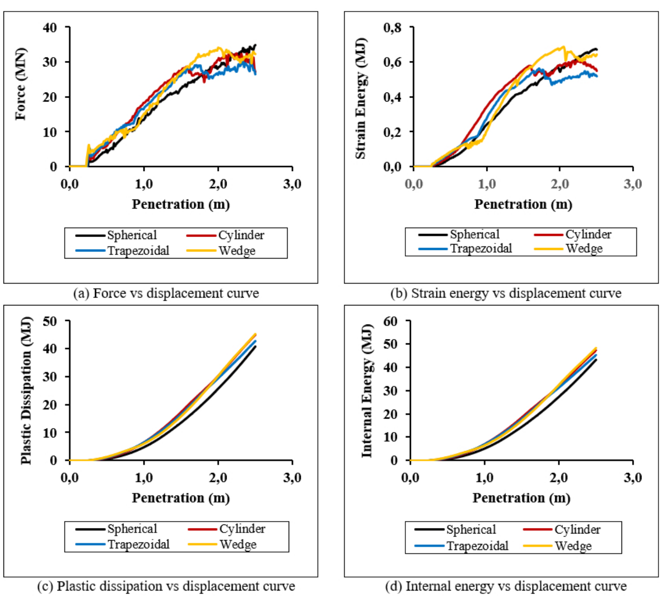

Source: Authors.

Fig 16 highlights the numerical results of the side shell under the impact of various bulbous bow shapes. Among the tested geometries, the spherical bulbous bow demonstrates the most favorable structural performance, as evidenced by its superior reaction force response. This improved performance can be attributed to the geometrical symmetry of the spherical bow, which facilitates a more uniform distribution of impact forces across the structure. The energy absorbed by the side shell due to strain is also highest for the spherical bulbous bow, demonstrating its effectiveness in distributing impact energy. Fig 16c and Fig 16d depict the plastic dissipation and internal energy curves, respectively. These curves reveal that the total energy absorbed by the side shell at 2.5 m/s collision speed is greater than that at 2 m/s, reflecting the increased kinetic energy at higher velocities. Unlike at lower collision speeds, where the inner hull remains unaffected due to limited penetration depths, the 2.5 m/s collision speed results in plastic deformation of the inner hull. This deformation contributes significantly to the overall reaction force and energy absorption of the hull structure, effectively enhancing the structural resilience of the ship. Fig 17 shows the penetration depth at which crack initiation occurs in the outer plate for different bulbous bow shapes. The spherical bulbous bow initiates cracks at a slightly greater penetration depth compared to other shapes, showcasing its ability to delay structural failure. This delayed cracking is attributed to the bow's geometrical symmetry, which promotes a more uniform distribution of strain and reduces localized stress concentrations.

Figure 17: Penetration depth at which crack occurs into the outer hull at 2.5 m/s collision velocity.

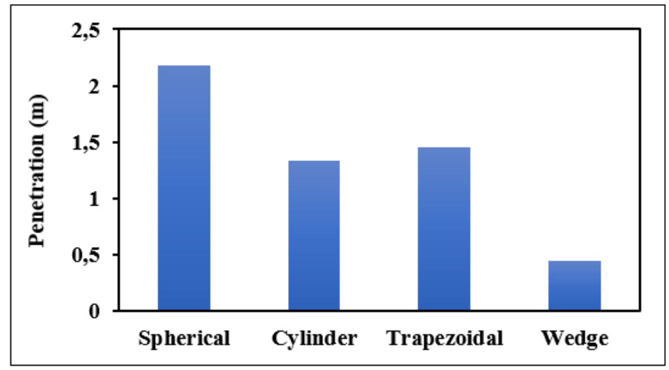

Source: Authors.

The curves in Fig 16 also indicate that the side shell continues to exert higher reaction forces even after crack initiation. This behavior can be explained by the presence of transverse frames located beneath the outer plate at the point of impact. These frames act as a secondary defense line, absorbing additional energy and enhancing the hull's resistance to further damage.

Figure 18: Maximum reaction force and absorbed energy before crack initiation at 2.5 m/s collision velocity.

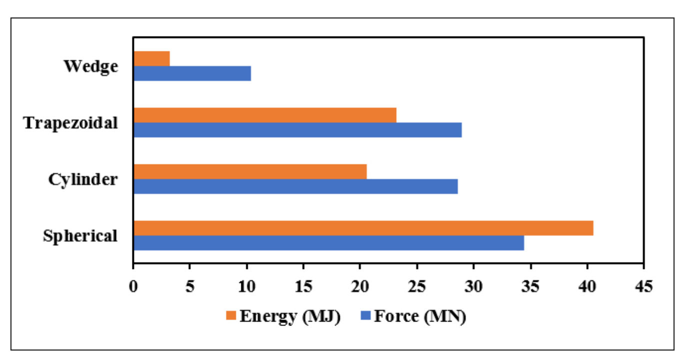

Source: Authors.

3.4. Results for 3 m/s collision velocity.

In this case, the collision is assumed to occur for 1 second and since the striking bow is rigid, so due to the offset distance of 250 mm the bow can penetrate up to 2.75 m through the side shell structure. The plastic strain, deformation and fracture are demonstrated for various simplified bow shapes. From the simulation results of double hull structure against different shaped bulbous bow it can be seen all the structural component of the side shell structure undergoes a plastic deformation and the outer hull, frames and inner hull finally rupture when the collision speed is 3 m/s (Fig. 19 & Fig. 20).

Figure 19: Deformation of outer hull under the impact of different bows at 3 m/s collision velocity.

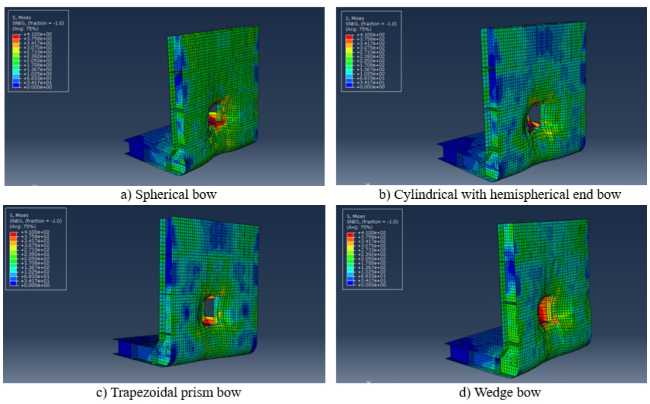

Source: Authors.

Figure 20: Deformation of inner hull under the impact of different bows at 3 m/s collision velocity.

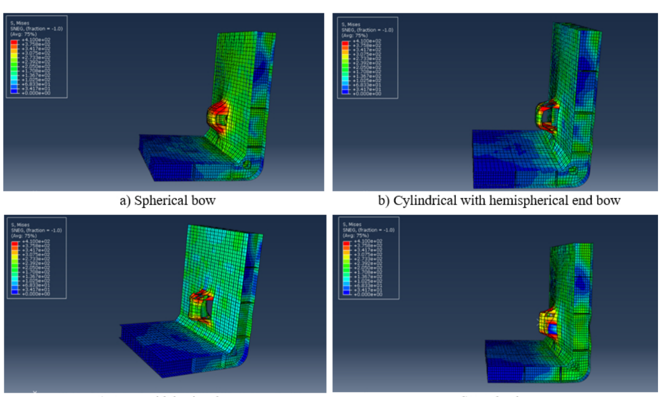

Source: Authors.

Fig 21 illustrates the numerical results of force-displacement and energy absorption-displacement curve of the double hull structure under various striking bows. The initial crack occurs at different penetration depth into the side shell structure for different bow shapes is shown in Fig 22. The force-penetration curve of numerical simulation for 3 m/s velocity of striking ship shows that the double hull structure can exert maximum reaction force in case of spherical shape striking bow before the initial crack occurs. The amount of reaction force is lower in case of rest of the simplified shaped striking bows i.e. cylindrical with hemispherical end, trapezoidal prism and wedge (Fig 23).

Figure 21: Numerical results of various striking bows at 3 m/s collision velocity.

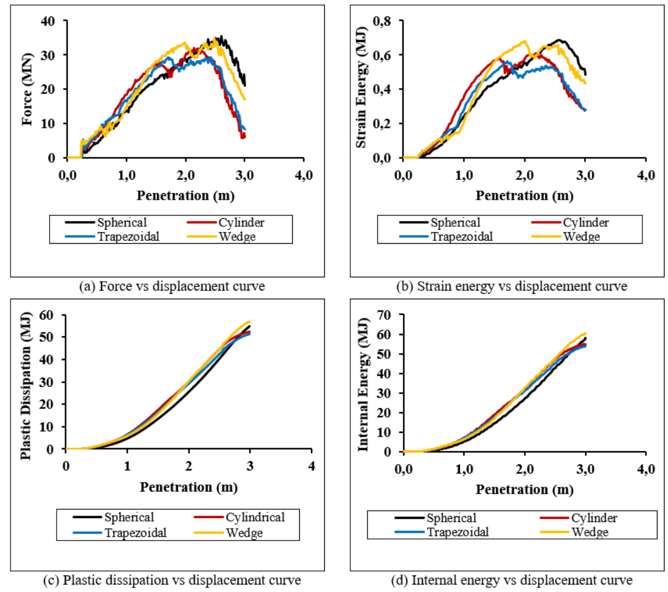

Source: Authors.

Figure 22: Penetration depth at which crack occurs into the outer hull at 3 m/s collision velocity.

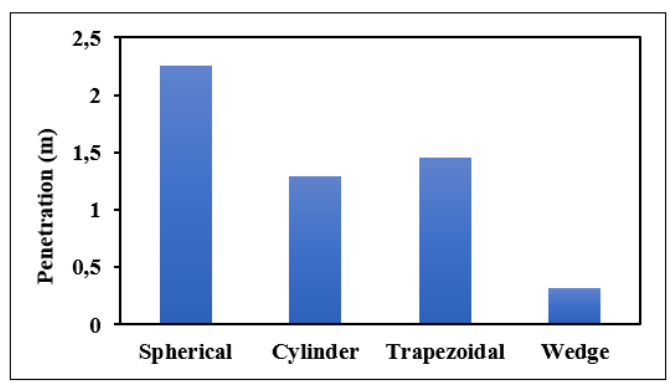

Source: Authors.

Figure 23: Maximum reaction force and absorbed energy before crack initiation at 3 m/s collision velocity.

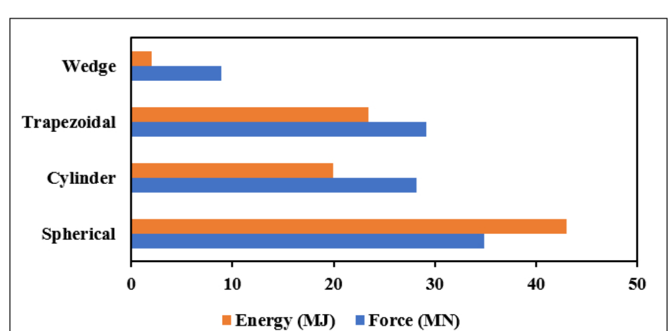

Source: Authors.

The energy absorption by the double hull structure is greater when struck with a spherical shape bulbous bow until fracture. When the trapezoidal prism shape, cylindrical with hemispherical end shape and wedge shape bulbous bow strikes the side shell of a ship hull structure, the hull structure can absorb less amount of energy compared to that of when struck with a spherical shape bulbous bow before the crack initiation (Fig 23).

In particular, structural discontinuities, such as stiffener terminations, bracket connections, and sudden cross - sectional changes in the hull, significantly influence the local stress concentration and damage initiation during impact [41], [42]. Large plastic deformations and membrane forces form in the outer plate beneath the wedge and trapezoidal prism strikers, especially at the striker's end corners. The outer plate cracks initially because to the considerable plastic strain localized at these places. Following that, the fracture spreads along the striker's contact to the outer plate's center (Fig. 24a and Fig. 24b).

Figure 24: Crack initiation in the outer hull under the impact of different striking bows.

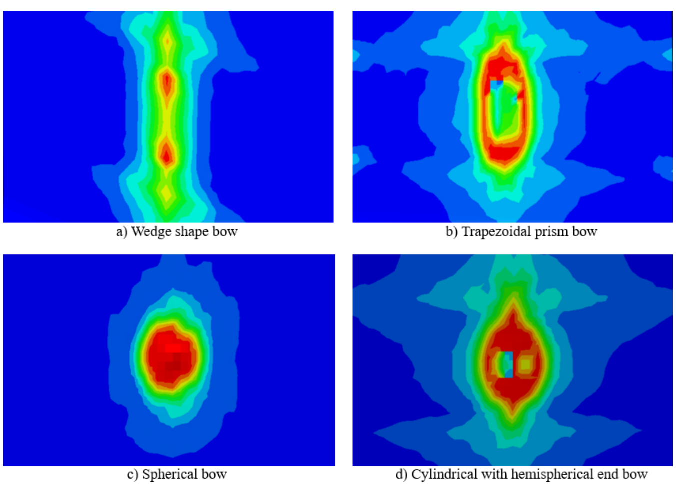

Source: Authors.

Figure 25: Structural members under the impact of spherical striking bow at 3 m/s collision velocity.

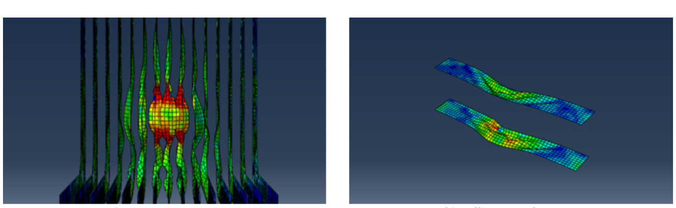

Source: Authors.

Global deflection and local indentation are the two components of the outer plate deformation in the case of a spherical striker. The striking head is shaped like the local depression. Because of the high in-plane tensile strain, the enormous impact energy initiates material rupture. A circular edge known as a necking circle is formed when the spherical striker penetrates the plate with ductile expansion, elongating the material in a plastic flow field beneath the striker.

The onset of fracture in the outer hull panels can be reasonably estimated using a localized necking-based fracture model that is largely mesh-insensitive. However, the numerical implementation of the necking and fracture model has a significant impact on the fracture propagation, particularly in situations where web frames and stringers are crushed [30]. Because of the limitations imposed by the stringers and web frames, the outer plate deforms axially. An axial membrane strain and related membrane force result from this stretching. Because of the membrane force at the necking circle, the plate thus experiences plastic deformation. The crack starts at the necking circle when the plate experiences significant plastic strain. Ultimately, as the striker enters the plate, the crack spreads radially along the necking circle (Fig. 24c).

Because both the cylindrical and spherical striker structures contain a circular cross-section, they experience identical deformation modes (Fig. 24d). The primary distinction is the local distortion brought on by the striker's shape. The ductile elongation of the material forms a necking ellipse below the striker. Initially, the cracks start at the antipodal points on the necking ellipse's principal axis and spread across the ellipse.

Fig 25 depicts the deformations of structural elements under the impact of spherical bulbous bow shapes. During the deformation process, the frames trip and fold (Fig. 25a). Since the shape of the striker changes along the vertical direction, this deformation also happens in the cases of spherical and cylindrical strikers. However, in the case of wedge and trapezoidal prism strikes, the frames undergo greater beam bending deformation.

In every instance, the stringer experiences the same deformation (Fig. 25b). Under local in-plane pressure, the stringer mostly experiences folding deformation. At a certain penetration, a complete fold forms, and it eventually flattens completely.

When the striking ship strikes the hull structure at a speed of 1.5 m/s, the inner panel does not undergo plastic deformation during the penetration and does not contribute to the energy dissipation of the double-hull construction. The primary cause of this phenomena is the fact that the height of the double-hull construction and the critical penetration at the outer panel fracture (about 1.25 m) are equal.

Fig 26 provides a detailed visualization of the maximum energy absorption by the hull structure when subjected to impacts from various striking bulbous bows at different collision velocities. At the lowest collision velocity of 1.5 m/s, the energy absorption is minimal. This is because the penetration depth of the bulbous bow into the side shell structure at this speed is relatively small. As the collision speed increases to 2 m/s, 2.5 m/s, and ultimately 3 m/s, the energy absorbed by the hull structure rises significantly. This increase is directly linked to the greater penetration depths achieved at higher velocities. At the maximum collision velocity of 3 m/s, the energy absorption reaches its peak. The penetration depth is the greatest at this speed, allowing the bulbous bow to engage more of the hull's material and structural elements. This results in a significant increase in both elastic and plastic deformation within the structure, maximizing the amount of energy that the hull can absorb before failure.

Figure 26: Energy absorbed by the side shell structure under different striking bows at varying collision velocities.

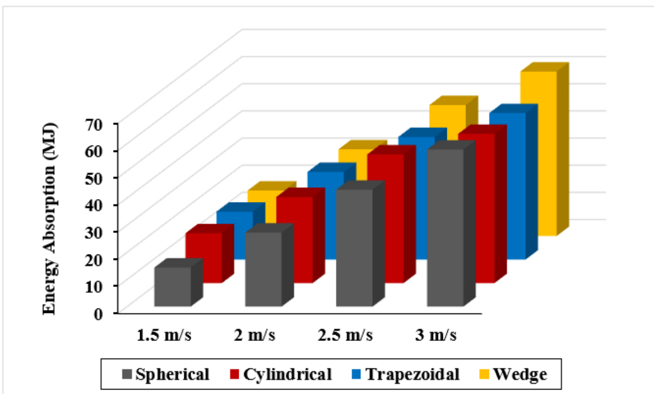

Source: Authors.

4. Analytical Analysis.

Without conducting real-world experiments, it is extremely difficult to validate this kind of serious damage to the ship hull structure from collisions and the related resistance force and energy absorption. The energy and resistance force during a dynamic impact into the ship hull can be predicted using a few analytical techniques. Minorsky[43] conducted a seminal analysis of 26 cases of full-scale ship collisions and developed an empirical formula to predict energy absorption by the structure during collision.

$$E = 47.2\, R_T + 32.7 \tag{1}$$

where R_T is the volume of damage material.

4.1. Energy Absorption Mechanism.

The assembly of the main deformation modes of the separate structural elements, such as web girders and stiffened panels, can be used to estimate the energy-absorbing mechanisms of double-hull structures [11]. The simplified analytical techniques can be used to evaluate their absorbed energy throughout the indentation process.

4.1.1. Energy Absorption by the Plate.

The energy absorbed by a plate during collision is governed by principles of material elongation and the formation of plastic hinges. A plate of thickness t_p and static yield stress σ_{yp} dissipates incident energy through membrane plastic tension and the rotation of plastic hinges [44] . Expressions for estimating the energy absorption of a single plate exposed to a flat edge indenter were developed by Cho and Lee [44]. According to Fig. 27(a), the plastic hinges form at all deformed angles θ_1, θ_2, θ_3, and θ_4, and the axial elongation takes place in the plate regions (I) and (II). Thus, Eqs. 2 and 3 indicate the energy absorbed by the plate membrane tension (U_{tp}) and the rotation of the plastic hinges (U_{bp}).

Figure 27: Deformed shape of structural members; Refs. *[44]*, *[45]*.

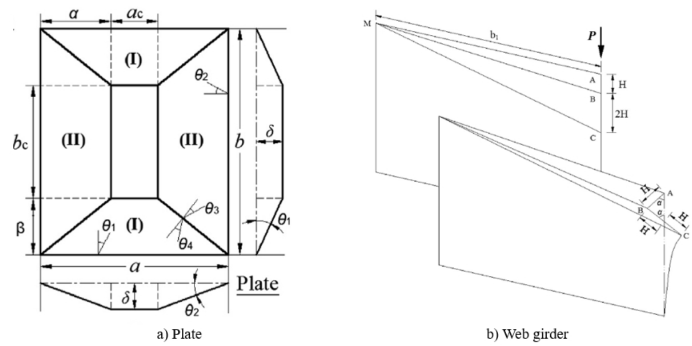

Source: Authors.

$$U_{tp} = 2\left(U_{tI} + U_{tII}\right) = 2\sigma_{yp} t_p \Big[(a_c + a_1)\Big(\sqrt{b_1^2 + \delta^2} - b_1\Big) + (b_c + b_1)\Big(\sqrt{a_1^2 + \delta^2} - a_1\Big)\Big] \tag{2}$$

$$U_{bp} = 0.5\, \sigma_{yp} t_p^2 \Big[(a + a_c)\theta_1 + (b + b_c)\theta_2 + 2\sqrt{a_1^2 + b_1^2}\,(\theta_3 + \theta_4)\Big] \tag{3}$$

$$\theta_1 = \arctan\left(\frac{\delta}{b_1}\right), \quad \theta_2 = \arctan\left(\frac{\delta}{a_1}\right), \quad \theta_3 = \arctan\left(\frac{\delta\, b_1}{a_1\sqrt{a_1^2 + b_1^2}}\right), \quad \theta_4 = \arctan\left(\frac{\delta\, a_1}{b_1\sqrt{a_1^2 + b_1^2}}\right) \tag{4}$$

The energy absorbed by the plate can be determined by

$$U_{\text{plate}} = U_{tp} + U_{bp} \tag{5}$$

4.1.2. Energy Absorption by Web Girders.

When subjected to impact loads, web girders exhibit a different damage pattern than plates.

Where the web girders sustain crushing and folding damage, the plate absorbs energy through tensile plastic damage. An analytical technique to determine the impact resistance of the webs under crushing was proposed by Liu and Soares [45].

$$H = 0.4436 b_w^{\frac{2}{3}} t_w^{\frac{1}{3}} \tag{6}$$

$$F(\delta)=\begin{cases}\dfrac{2}{3}\dfrac{\sigma_0\,t_w^2 b_w}{H\sqrt{1-\left(1-\dfrac{\delta}{3H}\right)}}+4\sigma_0 t_w H\,\dfrac{\delta}{b_w}, \qquad \delta\le 3H,\\ 3\sigma_0 t_w H\,\dfrac{2\delta-3H}{b_w}+\left(\dfrac{3}{2}\sigma_0 t_w^2 H+\dfrac{3}{2}\sigma_0 t_w H^2\right)\dfrac{1}{b_w}\dfrac{1}{1+\left(\dfrac{\delta}{b_w}\right)^2}\\ +\dfrac{\pi}{4}\dfrac{\sigma_0 t_w^2 b_w}{H}+2\sigma_0 t_w H\,\dfrac{\delta-3H}{b_w}, \qquad 3H\le\delta\le 5H,\\ 3\sigma_0 t_w H\,\dfrac{2\delta-3H}{b_w}+\displaystyle\sum_{i=1}^{n-2}2\sigma_0 t_w H\,\dfrac{2\delta-(4+4i)H}{b_w}\\ +\left(\dfrac{2n-1}{2}\sigma_0 t_w^2 H+\dfrac{(2n-1)^2}{2}\sigma_0 t_w H^2\right)\dfrac{1}{b_w}\dfrac{1}{1+\left(\dfrac{\delta}{b_w}\right)^2}\\ +\dfrac{\pi}{4}\dfrac{\sigma_0 t_w^2 b_w}{H}+2\sigma_0 t_w H\,\dfrac{\delta-(2n-1)H}{b_w},\\ (2n-1)H\le\delta\le(2n+1)H.\end{cases} \tag{7}$$

Where b_w is the half span length of web girder, t_w is the thickness of web, H is the folding wavelength of web and σ_0 is the material flow stress which is given by:

$$\sigma_0=\frac{\sigma_y+\sigma_u}{2} \tag{8}$$

By integrating the force penetration curve derived from the aforementioned equations, it is possible to estimate the energy absorption by the webs.

4.2. *Total Energy Absorption.*

By adding up the energy dissipated by the plate and the web girders, the Cho and Lee [44] technique and the Liu and Soares [45] approach can be used to determine the total energy absorbed by the hull structure. When there is less penetration and less substantial damage, this approach can be used.

Zhang and Pederson [10] updated the semi-analytical formula and presented a streamlined analytical technique to calculate the energy that the structure absorbs in relation to the volume of damaged material. Eq. 9 and can be used to determine the energy absorption by the plastic tension damage mode (E_1), such as outer hull.

$$E_1=0.77\epsilon_f\sigma_0 R_1 \tag{9}$$

where ϵ_f is the strain at rupture and R_1 is the material volume of the damaged structural member.

To calculate the energy absorption by the crushing and folding damage mode (E_2), such as girder and stringer Eq. 10 is used

$$E_2=3.50\left(\frac{t}{b}\right)^{0.67}\sigma_0 R_2 \tag{10}$$

where t is the crushed web thickness, b is the width of the member in crushed cross section and R_2 is the damage material volume of the crushed structural member.

and the total energy can be estimated by:

$$E_{total}=\sum E_1+E_2 \tag{11}$$

4.3. *Comparison with Numerical Result.*

In this study, numerical simulation results are compared with predictions from the combined method (Cho and Lee [44], Liu and Soares [45]) and the method developed by Zhang and Pederson [10] (Fig. 28). Energy absorption is evaluated using these approaches up to a penetration depth of 650 mm.

For small penetration depths, both analytical methods show good agreement with the numerical results. As penetration increases, slight deviations are observed between the numerical and analytical results. These deviations are primarily attributed to the moderate and coarse mesh sizes applied to structural members in simulations, which are used to optimize computational efficiency.

Notably, the numerical results continue to align closely with the predictions of the Zhang and Pederson [10] method even at penetration depths exceeding 500 mm. However, the combined method (Cho and Lee [44], Liu and Soares [45]) begins to deviate significantly from both the numerical results and Zhang and Pederson's predictions after this depth. This divergence highlights the limitations of the combined method in accurately capturing the extent and pattern of damage at higher penetration levels.

Conclusions.

This study examined into how a ship's side shell structure reacts when it collides with a bulbous bow. Through detailed computer simulations and analyses, valuable insights into the behavior of the materials and the potential damage is gained that may occur during such collisions. It is observed that certain factors, like the shape of the bow and the speed of impact, significantly influence the outcome.

Figure 28: Comparison between numerical and analytical result.

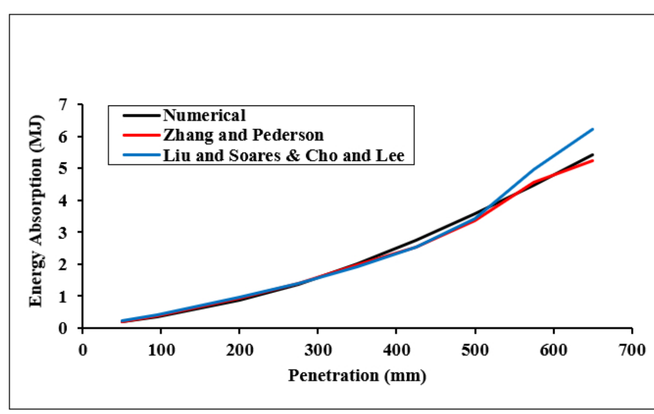

Source: Authors.

To analyze the structural response of a ship hull structure in a bow to side collision, a transverse framed double hull structure and various simplified shapes of bulbous bow i.e. spherical, trapezoidal prism, cylindrical with hemispherical end and wedge are modeled. The hull structure is struck with the different simplified shaped bulbous bow at different speeds i.e. 1.5

m/s, 2 m/s, 2.5 m/s and 3 m/s. The following conclusions are drawn after the numerical result of the analysis:

The double hull structure exerts better impact resistance towards the spherical shape bulbous bow as compared to the trapezoidal prism, cylindrical with hemispherical end and wedge shape bulbous bow. The energy absorption is much greater for the ship hull structure before it experiences the initial crack when subjected to spherical shape bulbous bow in comparison with trapezoidal prism, cylindrical with hemispherical end and wedge shape. The geometry of the striker strongly influences the structural plastic deformation and failure mechanism due to the contact area with the struck structure. Hence the better performing and the most effective bulbous bow shape is spherical shape in terms of structural damage due to collision.

Generally, this paper provides an important framework for assessing the strength of double-hull ship side structures during minor collisions. The findings highlight the importance of designing ship structures with a focus on energy absorption and deformation control. This can play an important role in minimizing damage and ensuring the safety of the vessel and its crew in the event of a collision.

This paper provides a strong foundation for further study on this subject. This study recommends the following topics as possibilities for future work: To reduce the computational time the meshes are used to the model of the structural members for the analysis is moderate and coarse mesh. The future work using the very fine mesh will provide more accurate result. The behaviors of the ship hull structure have been observed by varying the striker shape and the collision speed. Future work can be extended to investigate the structural response of the ship hull involving varying impact angles and materials. Due to the lack of sufficient actual ship collisions data, validation of the numerical result was much challenging. The study can be extended to undertaking extensive experimental studies to validate the findings of simulations. These studies could involve controlled collision experiments or data collection from actual maritime incidents.

Competing Interest.

The authors have no competing interests to declare that are relevant to the content of this article.

Acknowledgements.

The authors express their sincere gratitude to all individuals who contributed directly or indirectly throughout various stages of this work. Additionally, the authors acknowledge the support of the UGC HEQEP Sub-Project (CP#3131) "Strengthening the Research Capabilities and Experimental Facilities in the Field of Marine Structure" for providing access to the simulation lab facilities.

References.

[1] B. Liu, ‘Analytical method to assess double-hull ship structures subjected to bulbous bow collision’, Ocean Eng., vol. 142, pp. 27–38, Sep. 2017, doi: 10.1016/j.oceaneng.2017.06.062.

[2] S. J. Kim et al., ‘Comparison of numerical approaches for structural response analysis of passenger ships in collisions and groundings’, Mar. Struct., vol. 81, p. 103125, Jan. 2022, doi: 10.1016/j.marstruc.2021.103125.

[3] H. Liu, K. Liu, X. Wang, Z. Gao, and J. Wang, ‘On the Resistance of Cruciform Structures during Ship Collision and Grounding’, J. Mar. Sci. Eng., vol. 11, no. 2, Art. no. 2, Feb. 2023, doi: 10.3390/jmse11020459.

[4] I. Ladeira, L. Márquez, S. Echeverry, H. Le Sourne, and P. Rigo, ‘Review of methods to assess the structural response of offshore wind turbines subjected to ship impacts’, Ships Offshore Struct., vol. 18, no. 6, pp. 755–774, Jun. 2023, doi: 10.1080/17445302.2022.2072583.

[5] A. Rio Prabowo, D. Myung Bae, J. Min Sohn, A. Fauzan Zakki, B. Cao, and J. Hyung Cho, ‘Effects of the rebounding of a striking ship on structural crashworthiness during ship-ship collision’, Thin-Walled Struct., vol. 115, pp. 225–239, Jun. 2017, doi: 10.1016/j.tws.2017.02.022.

[6] M. T. Tavakoli, J. Amdahl, and B. J. Leira, ‘Analytical and numerical modelling of oil spill from a side tank with collision damage’, Ships Offshore Struct., vol. 7, no. 1, pp. 73–86, Mar. 2012, doi: 10.1080/17445302.2010.537844.

[7] Y. S. Kim et al., ‘Environmental consequences associated with collisions involving double hull oil tanker’, Ships Offshore Struct., vol. 10, no. 5, pp. 479–487, Sep. 2015, doi: 10.1080/17445302.2015.1026762.

[8] S. Haris and J. Amdahl, ‘An analytical model to assess a ship side during a collision’, Ships Offshore Struct., vol. 7, no. 4, pp. 431–448, Dec. 2012, doi: 10.1080/17445302.2011.614527.

[9] A. Obisesan, S. Sriramula, and J. Harrigan, ‘Probabilistic Considerations in the Damage Analysis of Ship Collisions’, in Numerical Methods for Reliability and Safety Assessment, S. Kadry and A. El Hami, Eds., Cham: Springer International Publishing, 2015, pp. 197–214. doi: 10.1007/978-3-319-07167-1_6.

[10] S. Zhang and P. T. Pedersen, ‘A method for ship collision damage and energy absorption analysis and its validation’, Ships Offshore Struct., vol. 12, no. sup1, pp. S11–S20, Mar. 2017, doi: 10.1080/17445302.2016.1254584.

[11] B. Liu, G. Wang, B. Chen, and C. Guedes Soares, ‘Experimental numerical and analytical analysis of the penetration of a scaled double-hull tanker side structure’, Mar. Struct., vol. 78, p. 103018, Jul. 2021, doi: 10.1016/j.marstruc.2021.103018.

[12] B. Liu and C. Guedes Soares, ‘Recent developments in ship collision analysis and challenges to an accidental limit state design method’, Ocean Eng., vol. 270, p. 113636, Feb. 2023, doi: 10.1016/j.oceaneng.2023.113636.

[13] S. Zhang, R. Villavicencio, L. Zhu, and P. T. Pedersen, ‘Ship collision damage assessment and validation with experiments and numerical simulations’, Mar. Struct., vol. 63, pp. 239–256, Jan. 2019, doi: 10.1016/j.marstruc.2018.09.005.

[14] B. Liu and C. Guedes Soares, ‘Analytical method to determine the crushing behaviour of girders with stiffened web’,

Int. J. Impact Eng., vol. 93, pp. 49–61, Jul. 2016, doi: 10.1016/j.ijimpeng.2016.02.008.

[15] A. R. Prabowo, H. Nubli, and J. M. Sohn, 'Energy Dissipation of Ship Structures subjected to Impact Loading: A Study Case in Side Collision', Procedia Struct. Integr., vol. 27, pp. 171–178, Jan. 2020, doi: 10.1016/j.prostr.2020.07.023.

[16] B.-Q. Chen, B. Liu, and C. Guedes Soares, 'Experimental and numerical investigation on a double hull structure subject to collision', Ocean Eng., vol. 256, p. 111437, Jul. 2022, doi: 10.1016/j.oceaneng.2022.111437.

[17] J. W. Ringsberg et al., 'MARSTRUCT benchmark study on nonlinear FE simulation of an experiment of an indenter impact with a ship side-shell structure', Mar. Struct., vol. 59, pp. 142–157, May 2018, doi: 10.1016/j.marstruc.2018.01.010.

[18] Z. Wang, K. Liu, G. Chen, and Z. Hu, 'An analytical method to assess the structural responses of ship side structures by raked bow under oblique collision scenarios', Proc. Inst. Mech. Eng. Part M J. Eng. Marit. Environ., vol. 235, no. 3, pp. 773–791, Aug. 2021, doi: 10.1177/1475090220980277.

[19] B. Liu and C. Guedes Soares, 'Experimental and numerical analysis of the crushing behaviour of stiffened web girders', Int. J. Impact Eng., vol. 88, pp. 22–38, Feb. 2016, doi: 10.1016/j.ijimpeng.2015.09.004.

[20] Y. G. Ko, S. J. Kim, J. M. Sohn, and J. K. Paik, 'A practical method to determine the dynamic fracture strain for the nonlinear finite element analysis of structural crashworthiness in ship–ship collisions', Ships Offshore Struct., vol. 13, no. 4, pp. 412–422, May 2018, doi: 10.1080/17445302.2017.1405584.

[21] Q. T. Do, T. Muttaqie, P.-T. Nhut, M. T. Vu, N. D. Khoa, and A. R. Prabowo, 'Residual ultimate strength assessment of submarine pressure hull under dynamic ship collision', Ocean Eng., vol. 266, p. 112951, Dec. 2022, doi: 10.1016/j.-oceaneng.2022.112951.

[22] M. Faisal et al., 'Rapid hull collapse strength calculations of double hull oil tankers after collisions', Ships Offshore Struct., vol. 12, no. 5, pp. 624–639, Jul. 2017, doi: 10.1080/17445302.2016.1192747.

[23] J. Weng, S. Liao, B. Wu, and D. Yang, 'Exploring effects of ship traffic characteristics and environmental conditions on ship collision frequency', Marit. Policy Manag., vol. 47, no. 4, pp. 523–543, May 2020, doi: 10.1080/03088839.2020.172-1584.

[24] M. Zhang, Z. Zhu, Y. Zeng, J. Liu, and Z. Hu, 'Analytical Method for Evaluating the Impact Response of Stiffeners in a Ship Side Shell Subjected to Bulbous Bow Collision', Math. Probl. Eng., vol. 2020, p. e5025438, Apr. 2020, doi: 10.1155/2020/5025438.

[25] Y. Zhang, Y. Yuan, J. Zhou, and W. Tang, 'A new analytical model to evaluate ship side collisions with large indentation considering interaction effects between structural components', Mar. Struct., vol. 95, p. 103596, May 2024, doi: 10.1016/j.marstruc.2024.103596.

[26] M. S. Islam, A. Z. Nayem, and K. N. Hoque, 'Finite element-based optimization procedure for an irregular domain with unstructured mesh', Heliyon, vol. 10, no. 4, Feb. 2024, doi: 10.1016/j.heliyon.2024.e25994.

[27] C. J. Sun, J. H. Zhou, and W. Wu, 'Study on Collision of Ship Side Structure by Simplified Plastic Analysis Method', IOP Conf. Ser. Mater. Sci. Eng., vol. 248, no. 1, p. 012028, Oct. 2017, doi: 10.1088/1757-899X/248/1/012028.

[28] B. Liu, R. Villavicencio, P. T. Pedersen, and C. Guedes Soares, 'Analysis of structural crashworthiness of double-hull ships in collision and grounding', Mar. Struct., vol. 76, p. 102898, Mar. 2021, doi: 10.1016/j.marstruc.2020.102898.

[29] Y. Okumoto, Y. Takeda, M. Mano, and T. Okada, Design of Ship Hull Structures: A Practical Guide for Engineers. Springer Science & Business Media, 2009.

[30] B. C. Cerik, S.-J. Park, and J. Choung, 'Use of localized necking and fracture as a failure criterion in ship collision analysis', Mar. Struct., vol. 73, p. 102787, Sep. 2020, doi: 10.1016/j.marstruc.2020.102787.

[31] X. Qiu, Y. Zhao, and D. Wang, 'Mechanical analysis and interior stiffeners arrangement discussion of a specific ship side collision situation', Ocean Eng., vol. 309, p. 118417, Oct. 2024, doi: 10.1016/j.oceaneng.2024.118417.

[32] U. B. Karlsson, J. W. Ringsberg, E. Johnson, M. Hoseini, and A. Ulfvarson, 'Experimental and Numerical Investigation of Bulb Impact with a Ship Side-Shell Structure', Mar. Technol. SNAME News, vol. 46, no. 01, pp. 16–26, Jan. 2009, doi: 10.5957/mtsn.2009.46.1.16.

[33] A. Kuznecovs, J. W. Ringsberg, E. Johnson, and Y. Yamada, 'Ultimate limit state analysis of a double-hull tanker subjected to biaxial bending in intact and collision-damaged conditions', Ocean Eng., vol. 209, p. 107519, Aug. 2020, doi: 10.1016/j.oceaneng.2020.107519.

[34] J. Parunov, P. Prebeg, and S. Rudan, 'Post-accidental structural reliability of double-hull oil tanker with near realistic collision damage shapes', Ships Offshore Struct., vol. 15, no. sup1, pp. S190–S207, Dec. 2020, doi: 10.1080/17445302.20-20.1789035.

[35] Z. Wang, C. Guo, C. Wang, G. Chen, Y. Xu, and Q. Li, 'An analytical method for predicting the structural response of ship side structures by bulbous bow in oblique collision scenarios', Ships Offshore Struct., vol. 0, no. 0, pp. 1–14, doi: 10.1080/17445302.2023.2247839.

[36] Y. Yu, D. Zhao, C. Li, Y. Liang, Z. Wang, and W. Sun, 'Research on ship-ice collision model and ship-bow fatigue failure mechanism based on elastic-plastic ice constitutive relation', Ocean Eng., vol. 306, p. 118005, Aug. 2024, doi: 10.1016/j.oceaneng.2024.118005.

[37] L. Wang, L. Yang, D. Huang, Z. Zhang, and G. Chen, 'An impact dynamics analysis on a new crashworthy device against ship–bridge collision', Int. J. Impact Eng., vol. 35, no. 8, pp. 895–904, Aug. 2008, doi: 10.1016/j.ijimpeng.2007.12.-005.

[38] Pu Q, Liu J, Gou H, Bao Y, Xie H. Finite element analysis of long-span rail-cum-road cable-stayed bridge subjected to ship collision. Advances in Structural Engineering. 2019;22(11):2530-2542. doi:10.1177/1369433219846953

[39] A. J. Brown, 'Collision scenarios and probabilistic collision damage', Mar. Struct., vol. 15, no. 4, pp. 335–364, Jul. 2002, doi: 10.1016/S0951-8339(02)00007-2.

[40] B. Liu, R. Villavicencio, and C. Guedes Soares, 'Experimental and Numerical Plastic Response and Failure of Laterally Impacted Rectangular Plates', J. Offshore Mech. Arct. Eng., vol. 135, no. 041602, Jul. 2013, doi: 10.1115/1.4024274.

[41] K. N. Hoque and M. S. Islam, 'Finite element approach to analyze structural discontinuities associated with ship hull', J. Nav. Archit. Mar. Eng., vol. 20, no. 3, Art. no. 3, Dec. 2023, doi: 10.3329/jname.v20i3.69756.

[42] K. N. Hoque and M. S. Islam, 'Stress-strain analysis of structural discontinuities associated with ship hulls', J. Nav. Archit. Mar. Eng., vol. 20, no. 1, Art. no. 1, Jun. 2023, doi: 10.3329/jname.v20i1.58298.

[43] V. U. Minorsky, 'An Analysys of Ship Collision to Protection of Nuclear Powered Plant.', J. Ship Research, 1959.

[44] S.-R. Cho and H.-S. Lee, 'Experimental and analytical investigations on the response of stiffened plates subjected to lateral collisions', Mar. Struct., vol. 22, no. 1, pp. 84–95, Jan. 2009, doi: 10.1016/j.marstruc.2008.06.003.

[45] B. Liu and C. Guedes Soares, 'Simplified analytical method for evaluating web girder crushing during ship collision and grounding', Mar. Struct., vol. 42, pp. 71–94, Jul. 2015, doi: 10.1016/j.marstruc.2015.03.001.